Full paper/Mémoire

Preparation, characterization and application of a CTAB-modified nanoclay for the adsorption of an herbicide from aqueous solutions: Kinetic and equilibrium studies

Mehdi Shirzad-Siboni [a,b], Alireza Khataee [c,*], Aydin Hassani [d,e], Semra Karaca [d]

[a] Department of Environmental Health Engineering, School of Health, Guilan University of Medical Sciences, Rasht, Iran
[b] Department of Environmental Health Engineering, School of Public Health, Iran University of Medical Sciences, Tehran, Iran
[c] Research Laboratory of Advanced Water and Wastewater Treatment Processes, Department of Applied Chemistry, Faculty of Chemistry, University of Tabriz, Tabriz, Iran
[d] Department of Chemistry, Faculty of Science, Atatürk University, 25240 Erzurum, Turkey
[e] Photochemical Nanosciences Laboratory, Department of Chemistry "G. Ciamician", University of Bologna, Via Selmi 2, 40126 Bologna, Italy

A B S T R A C T

In this study, surfactant-modified pillared montmorillonites (MMT) were prepared using cetyltrimethylammonium bromide (CTAB) by the intercalation method and used as adsorbent to remove bentazon from aqueous solutions. The main compositions of MMT and CTAB/MMT were characterized by Fourier transform–infrared spectroscopy (FT–IR), X-ray diffraction (XRD), scanning electron micrography (SEM) and energy dispersive X-ray (EDX) spectroscopy. The removal efficiency of bentazon was studied as a function of adsorbent dosage, pH, initial bentazon concentration and ionic strength (sodium carbonate, sodium bicarbonate, sodium sulfate and sodium chloride). The removal efficiency of bentazon by CTAB/MMT was more than that of MMT in similar conditions. By increasing adsorbent dosage and initial bentazon concentration, the removal efficiency was increased and declined, respectively. The results showed that the maximum adsorption of organo-modified montmorillonite was obtained at pH 3. The maximum adsorption capacity was estimated to be 500 mg/g at pH 3 and room temperature. The study of the adsorption kinetic model revealed that the pseudo-second order model was the best applicable one to describe the adsorption of bentazon onto CTAB/MMT. Adsorption data were analyzed by both Langmuir and Freundlich adsorption isotherms and the results showed that it was better described by the Langmuir model. The adsorption capacities of the samples were found to increase with Na_2CO_3 anion saturation, while they decreased in the presence of $NaHCO_3$, Na_2SO_4 and $NaCl$.

© 2014 Académie des sciences. Published by Elsevier Masson SAS. All rights reserved.

1. Introduction

Diffused groundwater contamination by herbicides has generated environmental and toxicological problems, which have resulted in a large number of studies to recognize the factors that influence the fate of agrochemicals in soils [1,2]. Using of herbicides is vital in order to increase agricultural productivity [3]. A wide variety of herbicides is introduced into the aquatic environments from diverse sources, such as chemical spills, industrial effluents and agricultural run-offs. Their perdurability, stability and toxicity in the environment cause much concern to regulation authorities and environmental protection societies. The discharge of wastewater-containing herbicides to receiving streams affects the aesthetic

---

* Corresponding author.
  E-mail addresses: a_khataee@tabrizu.ac.ir, ar_khataee@yahoo.com
 (A. Khataee).

value of environment. Bentazon is a widely used herbicide usually applied for the control of broad-leaf weeds and sedges in many crops, such as beans, corn, rice, peanuts and peas [4,5]. It is harmful, if it is swallowed or absorbed through the skin and causes irritation to the eyes. It is classified as toxicity class III, slightly toxic, and dangerous for the environment [6]. The maximum permissible concentration of bentazon in drinking water is 30 g/L [7,8]. To achieve cleanup purposes, various physicochemical procedures have been provided for the treatment of water and wastewater-containing herbicide wastes, such as photodegradation [9], photocatalytic degradation [10], oxidation by ozone [11], removal by zeolite [12], ultrasonic irradiation [13] and adsorption [14,15]. It is now extensively recognized that sorption processes provide a feasible method for the removal of herbicide from water and wastewater. Adsorption has been found to be superior compared to other methods for wastewater treatment due to its capability to efficiently remove a wide range of pollutants, low cost, simplicity of design, ease of operation and impassibility of toxic substances [14,16–18]. Adsorption on activated carbons is a widely used process for organic contaminants removal [19–21]. It can be described as a crude form of graphite, and a broad range of pore sizes, porous nature of this adsorbent material are favourable properties for adsorption. However, high cost and recovering problems of activated carbon particles from treated water are of disadvantages. Some studies have shown the importance of low cost materials modified by chemical or physical processes as adsorbents for removal of organic pollutants from water and wastewater [22,23]. Recently organo-nanoclays have been characterized for their immense ability to remove herbicide [24–27] and it showed that they were a powerful sorbent. Clay minerals and modified nanoclay minerals are good candidate adsorbents for the treatment of environmental contaminants due to their exclusive features, such as abundance, high specific surface areas, inexpensive availability, environmental stability, high adsorptive and ion exchange properties [22,24,28–30]. They could be used as adsorbent for the removal dangerous pollutants after surface modification with organic cations [3,30–32]. Among the studied clays for the adsorption of herbicide, expandable layered silicates for instance montmorillonite (MMT) with negative charge have received much more attention because they are available, relatively cheap, easily extracted, non-toxic and mechanically and chemically stable [33]. However, the application of pure MMT clay is not efficient for removing anionic herbicide, such as bentazon from aqueous media. Thus, chemical modification of pure MMT with an appropriate chemical agent would be favorable to reach suitable surface charge in order to increase adsorption capacity of the clay [34–37]. The modification of MMT surface by using cationic surface active substances, such as cetyltrimethylammonium bromide (CTAB) can change its surface properties, such as surface charge, hydrophobicity and cation-exchange capacity.

Hence, in this paper, the adsorption of bentazon using MMT modified with CTAB was considered in aqueous solutions. To the best of our knowledge, there is no report on the application of CTAB intercalated nano-sized MMT for removing bentazon as an anionic herbicide from aqueous media. The effects of adsorbent dosage, pH, initial herbicide concentrations and ionic strength (sodium carbonate, sodium bicarbonate, sodium sulfate and sodium chloride) for different time intervals on the removal efficiency were studied. Adsorption isotherm and kinetic studies were undertaken to comprehend the adsorption mechanism and maximum adsorption capacity of CTAB/MMT.

2. Materials and methods

2.1. Chemicals

The MMT nanoclay was K10 grade purchased from Sigma–Aldrich Co. (USA) with a surface area of 279.28 ± 0.846 m^2/g. Cetyltrimethylammonium bromide (CTAB) with chemical formula of $C_{19}H_{42}BrN$ and molecular weight of 364.46 g/mol as the surfactant was purchased from Merck, Germany. Its critical micelle concentration (CMC) is 328 mg/L [38]. All others chemicals and reagents were of analytical grade purchased from Merck, Germany. Bentazon [3-isopropyl-1H-2,1,3-benzothiadiazin-4 (3H)-one-2,2-dioxide] as a model herbicide was obtained from Chem-service (USA). Its chemical structure and other characteristics are listed in Table 1.

2.2. Preparation of CTAB intercalated MMT nanomaterial

The cation-exchange capacity (CEC) of the MMT-K10 (120 m_{eq}/100 g) was determined by the dye adsorption method as described in the literature [39]. The synthesis of CTAB-modified MMT was conducted by the following procedure. An amount of 1 g MMT was first dispersed in 100 mL of distilled water for 24 h at room temperature using a magnetic stirrer to swell and to reach homogeneity. Then, a desired amount of CTAB (0.44 g), which is 1.0 times CEC of montmorillonite was slowly added. The reaction mixture was stirred for 5 h, then stirring was stopped and

Table 1
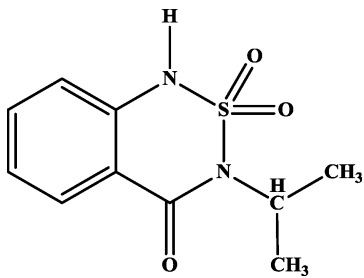The structure and characteristics of herbicide.

Structure

Formula	$C_{10}H_{12}N_2O_3S$
λ_{max} (nm)	335
M_w (g/mol)	240.3
Solubility in water (g/L)	0.50

Fig. 1. The modification procedure of nanoclay with CTAB.

the resultant organoclay was filtered and washed with distilled water for several times until it became free from excess salts and dried at 90 °C in an oven. The product was ground and sieved using standard sieves to obtain chemically modified adsorbent. The hypothetical simulating of the modification of MMT with CTAB is depicted in Fig. 1. Also, the point of zero charge (pH$_{zpc}$) of adsorbent was determined. Adsorbent (0.2 g) was added to 50 mL of 0.1 M NaNO$_3$ solutions at various initial pH between range of 3 to 10. The initial pH of solutions were adjusted by the addition of 0.1 M NaOH or HCl, and measured by pH meter (Metron, Switzerland). Afterward, the mixtures were shaken on a rotary shaker (KS-15, Edmund Buhler, Germany) at 150 rpm for 48 h at room temperature and the final pH of each solution was measured at equilibrium.

2.3. Characterization instruments

The X-ray diffraction (XRD) studies were performed with a Philips XRD instrument (Siemens D-5000, Germany) using Cu Kα radiation (λ = 1.5406 Å) at wide-angle range (2θ value 4–70°), the accelerating voltage of 40 kV and the emission current of 30 mA. For characterization of the functional groups on the surface of the samples, Fourier transform–infrared spectroscopy (FT–IR) spectra were recorded on a PerkinElmer (Germany) spectrometer under a dry air at room temperature by the KBr pellets method. The spectra were collected over the range from 4000 to 400 cm^{-1}. The surface morphology of MMT and organo-MMT were obtained by a TESCAN microscope (Model: MIRA3, Czech Republic). SEM images were further supported by energy dispersive X-ray (EDX) microanalysis to provide direct evidence for the purity, existence and distribution of specific elements in a solid sample.

2.4. Adsorption experiments

The adsorption experiments were carried out in 1000 mL Erlenmeyer flask containing 20 mL of bentazon solution and 0.5 g of CTAB/MMT powder, while the mixtures were stirred at 150 rpm and room temperature (25 ± 2 °C) in different time intervals (0–90 min). Then, the samples were centrifuged (Sigma-301, Germany) at 4000 rpm for 15 min to remove the adsorbent. The concentration of the bentazon in each sample was measured using a spectrophotometer (UV–Vis Spectrophotometer, Hach-DR 5000, USA) at λ_{max} = 335 nm by a calibration curve, which was depicted based on Beer–Lambert law.

In order to determine the effects of various parameters, the experiments were conducted by different adsorbent amounts of 0.05 to 0.5 g/L, initial bentazon concentrations of 10 to 100 mg/L and initial pH of 3 to 11. The amount of bentazon adsorbed by the CTAB/MMT and the bentazon removal efficiency were calculated through Eqs. (1) and (2), respectively.

$$q = \frac{(C_0 - C_e)V}{M} \times 100 \qquad (1)$$

$$\text{Removal efficiency } (\%) = \frac{(C_i - C_0)}{C_i} \times 100 \qquad (2)$$

where, q is the adsorption capacity (mg/g), C_i, C_0 and C_e are the initial, outlet and equilibrium concentrations of bentazon (mg/L), V is the volume of bentazon solution (L) and M is the total amount of CTAB/MMT (g).

Adsorption kinetic experiments were carried out by agitating bentazon solutions (10, 20, 40, 80 and 100 mg/L) containing 0.5 g/L of CTAB/MMT powder for various contact times (2–90 min) at pH 3 and room temperature (25 ± 2 °C). The pseudo-first-order and pseudo-second-order models were selected in order to find an efficient model for the best kinetically description of adsorption, the relevant equations can be considered as Eqs. (3) and (4), respectively [40,41].

$$\log(q_e - q_t) = \log q_e \left(\frac{k_1}{2.303}\right)t \qquad (3)$$

$$\frac{t}{q_t} = \left(\frac{1}{k_2 q_e^2}\right) + \left(\frac{1}{q_e}\right)t \qquad (4)$$

where q_e and q_t are the amounts of the bentazon adsorbed by CTAB/MMT (mg/L) at the equilibrium and after a time t, respectively, and k_1 (1/min) and k_2 (g/mg min) are the pseudo-first-order and pseudo-second-order rate constants, respectively.

To investigate the adsorption equilibrium isotherm, the experiments were performed with 20 mg/L initial concentration of bentazon using various adsorbent dosages (0.01–0.2 g/L) at pH 3 for 24 h. All experiments were repeated in three times and the average values were reported. The commonly used isotherm equation, namely Langmuir and Freundlich were applied to equilibrium data, and the related equations are described by Eqs. (5) and (6), respectively.

$$q_e = \frac{K_L q_m C_e}{1 + K_L C_e} \qquad (5)$$

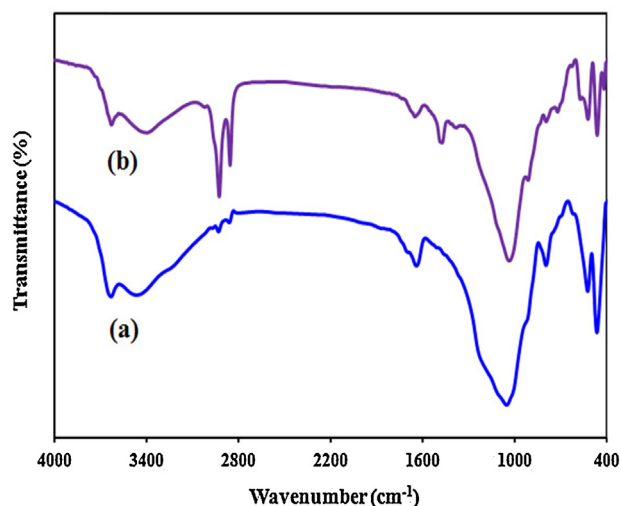$$\log q_e = \log K_F + \frac{1}{n} \log C_e \qquad (6)$$

Fig. 2. FT–IR patterns of samples; (a) MMT, and (b) CTAB/MMT.

where q_m (mg/g) is maximum monolayer adsorption capacity, C_e is the sorbate concentration in solution at equilibrium (mg/L), K_L (L/mg) and K_F ($mg^{1-1/n} L^{1/n} g^{-1}$) are the Langmuir and Freundlich constants, respectively, and n is the intensity of adsorption [42–44].

3. Results and discussion

3.1. Characterization of the adsorbent

The FT–IR spectra of pure MMT and the MMT-containing CTAB were shown in Fig. 2. A relatively small band around 3626 cm^{-1} was attributed to the Al_2OH group of the octahedral layer from the IR spectra of MMT [45]. A broad band around 3463 cm^{-1} was ascribed to the overlapping symmetric and asymmetric hydroxyl group stretching vibration of water molecules on the external layer [46]. The band around 1053 cm^{-1} was attributed to asymmetric stretching vibration of Si–O–Si tetrahedra in the MMT [47]. Comparison of FT–IR spectra of CTAB/MMT with that of pure MMT exhibits significant changes in some of the peaks (Fig. 2). In particular, the shift in the siloxan peak from 1053 cm^{-1} to 1037 cm^{-1} after loading of CTAB highlights the role of siloxan group in the adsorption of surfactant onto the MMT surface. [47,48]. From the IR spectra of the organocaly (CTAB/MMT), the adsorption band observed around 3631 cm^{-1} corresponding to the stretching vibration of the hydroxyl group and the interlayer water molecules was observed. Bending vibration of water molecules causes a peak around 1629 cm^{-1}. Also, the additional peaks at 2800–3000 cm^{-1}, appointed to –CH–stretching vibration, could be observed in CTAB/MMT. The appeared peaks in CTAB/MMT nanomaterial at 2926 cm^{-1} and 2854 cm^{-1} absent in the FT–IR spectrum of the pristine MMT indicate the incorporation (or the presence) of the surfactant and their intensity may be use in order to estimate the increase of adsorbed amount of surfactant. Additionally, the band at

3460 cm^{-1} was disappeared after the modification of MMT nanomaterial with CTAB, which indicates the removal of water molecules and the change in the hydrophobicity of MMT nanomaterial. It has been reported that the ordered conformation of the alkyl chains in the confined system has a strong dependence on amine concentration and orientation [47,49]. In relatively high concentration range, the confined amine chains adopt an essentially all-trans conformation and the frequency of the asymmetric CH_2 stretching absorption band locates at a relatively low frequency. However, in the relatively low amine concentration range, the frequency shifts significantly to high frequency and the confined amine chains adopt a large number of gauche conformations. Only when the chains are highly ordered (all-trans conformation), the narrow absorption bands appear around 2918 cm^{-1} asymmetric CH_2 and 2850 cm^{-1} symmetric CH_2 in the infrared spectrum. If conformational disorder is included in the
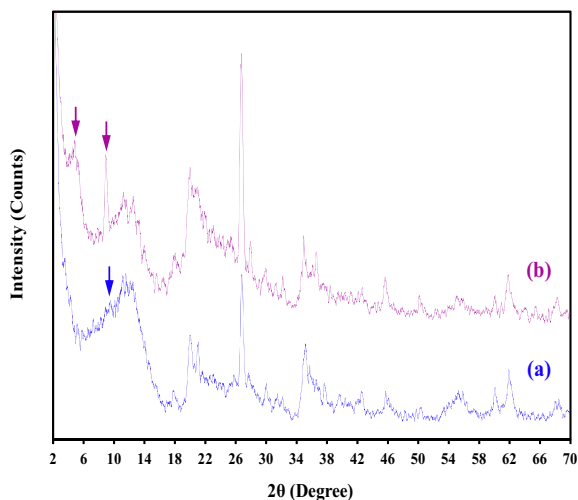

Fig. 3. XRD images of samples; (a) MMT, and (b) CTAB/MMT.

chains, their frequencies shift upward, depending upon the average content of gauche conformers. As shown in Fig. 2, with loading of surfactant asymmetric (CH$_2$) shifts from 2927 to 2922 cm^{-1} and symmetric (CH$_2$) shifts slightly from 2856 to 2852 cm^{-1} for the CTAB/MMT organoclay. This suggests that, in the presence of added surfactant, the confined surfactant chains adopt an essentially all-trans conformation. This result clearly reveals that the surface modification of MMT is achieved by surfactant.

XRD patterns of pristine MMT and CTAB/MMT sample are shown in Fig. 3. Montmorillonite clay sample has 2:1 layered structure of smectite class. As seen in Fig. 3, with an addition of surfactant, the basal spacing of the resultant organoclay increases indicating location of CTA$^+$ ions between layers of clay and resulting in a decrease of the hydration water content. So, the surface property changes from hydrophilic to hydrophobic. As known, the amount of added surfactant has a direct effect on the interlayer expansion of smectites [49]. Decrease in intensity of the main peak in $2\theta = 9.36°$ (0.944 nm) belonging to MMT and appeared two new peaks in $2\theta = 4.7°$ ($d = 1.878$ nm) and $2\theta = 8.88°$ ($d = 1.004$ nm)
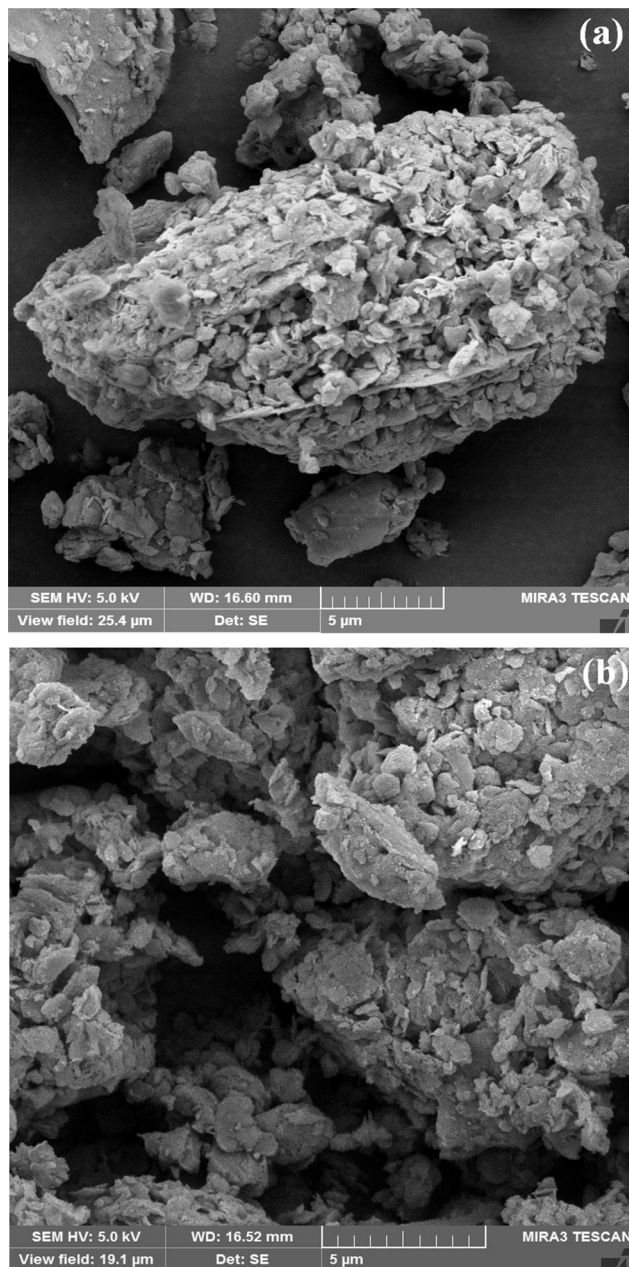

Fig. 4. SEM images of samples; (a) MMT, and (b) CTAB/MMT.

in CTAB/MMT sample show two different arrangement of CTAB interlayer galleries of clay.

SEM analysis was carried out to evaluate surface morphology of the unmodified and modified MMT and the results are depicted in Fig. 4. As it is shown, the figure reveals that the surface morphologies of both MMT samples are different and both unmodified and modified MMT have uneven structure with non-uniform size distribution. The montmorillonite shows massive, aggregated morphology, and some large flakes were observed in some instances. After modification with polymeric species, the clay surface was changed to a non-aggregated morphology and there are a large number of small flakes with severely crumpled structures. Furthermore, the surface of modified MMT was expanded due to the chemical intercalation with CTAB (Fig. 4b). An expanded interlayer for CTAB intercalated MMT nanomaterial would be appropriate place for a chemical reaction like interlayer exchange and interlayer adsorption. It has been demonstrated that the surfactant intercalated MMT nanomaterial exhibits a larger pore size and specific surface area than the pure MMT. Also, composition of the adsorbent was evaluated using EDX analysis and the result is showed in Fig. 5. Based on the EDX micrograph, the major portion of the modified MMT nanomaterial is composed of Si compounds, which are suitable for the adsorption of various organic pollutants, such as organic herbicide from aqueous solution. The weight percentages (wt%) of Si, O, Al, C, Fe, Mg and K compounds within the adsorbent were 44.42, 32.50, 9.10, 8.46, 3.23, 1.57 and 0.70%, respectively.

3.2. The effect of operational parameters on the bentazon removal efficiency

3.2.1. The effect of adsorbent dosage and contact time

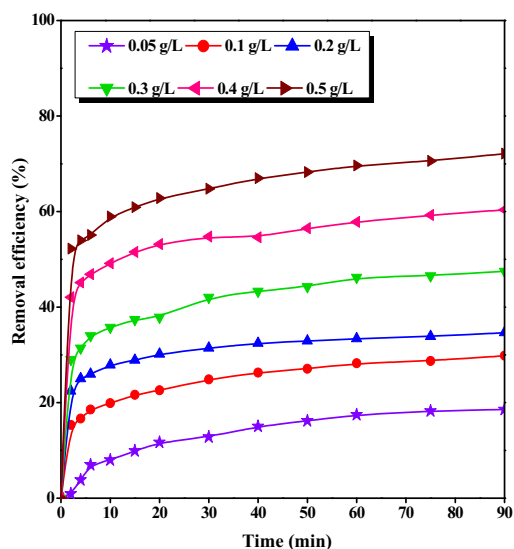The influence of adsorbent dosage on the adsorption efficiency was investigated for six various amounts in the

Fig. 6. The effect of adsorbent dosage on the removal of bentazon by CTAB/MMT for different time intervals for ([Bentazon]$_0$ = 20 mg/L, and pH = 7).

range of 0.05–0.5 g/L in pH = 7 at different time intervals (Fig. 6). It was evident that the bentazon removal efficiency was increased by increasing the adsorbent dosage from 0.05–0.5 g/L for different time intervals (2–90 min). The increasing of removal efficiency with an increase in the adsorbent dosage was as a result of the presence of a high surface area and consequently more number of available sites for adsorption.

As can be seen in Fig. 6, the rate of removal of bentazon at all dosages is primarily rapid in the first stages of contact time and then it is gradually slowed until reactions reach equilibrium at about 90 min. After the increase in the exposure, time has a negligible effect on the efficiency of adsorption process. The rapid adsorption observed during
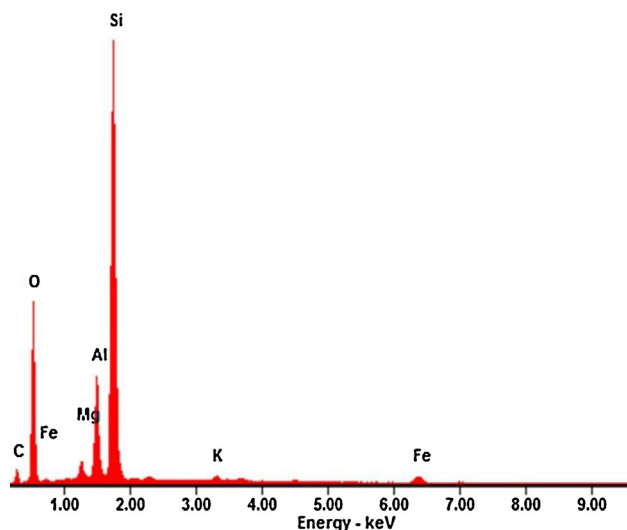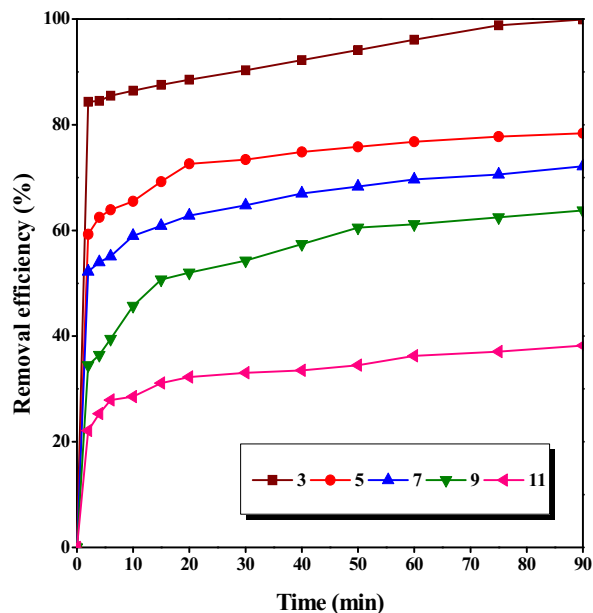
Fig. 5. EDX of CTAB/MMT sample.

Fig. 7. The effect of pH on the removal of bentazon by CTAB/MMT in different time interval ([Bentazon]$_0$ = 20 mg/L, and adsorbent dosage = 0.5 g/L).

the first times of process was attributed to the abundance of free active sites on the CTAB/MMT surface and easy availability of them for bentazon molecules. Subsequently, a decrease in the active sites is due to their occupation by bentazon molecules and other hand repulsive forces among the adsorbed bentazon molecules on the CTAB/MMT and bulk phase reduction in the rapid of adsorption process.

3.2.2. The effect of pH of the solution

The effect of pH on the variation of bentazon adsorption onto CTAB/MMT was investigated for pH ranging between 3 and 11 and the results are depicted in Fig. 7. According to Fig. 7, the pH of a solution is recognized as a very impressive parameter that governs the adsorption process. Generally, it is established that pH affects the surface charge of the adsorbent. The removal efficiency of bentazon decreased with increase in the initial solution pH. It may be due to hydrolysis of the adsorbent in water, which can create positively charged sites and increase in electrostatic repulsion between bentazon ions and CTAB/MMT surface with increase in pH. Percentage removal of bentazon was maximum at the initial pH of 3.0 (99.93%). Bentazon is a weak acid with pK$_a$ of 3.3; and at pH above the pK$_a$, it is predominantly in anionic form. In order to obtain information about the surface charge of the adsorbent, the point of zero charge (pH$_{ZPC}$) was determined. The plot of ΔpH versus pHi of the solutions is illustrated in Fig. 8. It can be seen that pH$_{ZPC}$ i.e. the pH at which the net surface charge on MMT/CTAB was zero (ΔpH = 0) corresponds to a pH value around 4.4. This means that at pH values below 4.4 the CTAB/MMT surface has a net positive charge, while at pH greater than 4.4, the surface has a net negative charge. Hence, the acidic pH facilitates the adsorption of anionic bentazon onto CTAB/
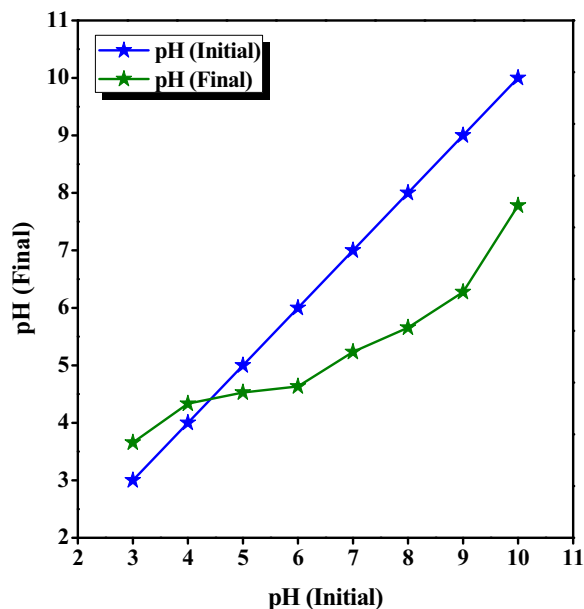
MMT surface, as maximum removal of bentazon obtained at pH 3 [50,51].

3.2.3. The effect of initial bentazon concentration

The adsorption of bentazon by CTAB/MMT was investigated by varying its initial concentrations (10, 20, 40, 80 and 100 mg/L) at initial pH of 3.0 for different time intervals (Fig. 9). When the initial bentazon concentration was increased from 10 to 100 mg/L, the bentazon removal efficiency was decreased from 99.99% to 28.48%. The
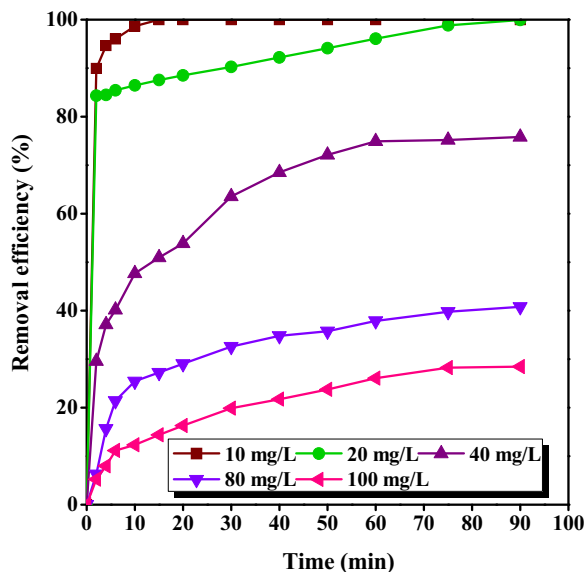

Fig. 8. Determination of the pH of point of zero charge (PZC).

Fig. 9. The effect of initial bentazon concentration on the removal of herbicide by CTAB/MMT in different time interval (pH = 3, and adsorbent dosage = 0.5 g/L).

reason for this result can be explained with the fact that the adsorbent has a limited number of active sites, which would become saturated above a certain bentazon concentration. Similar observations were also reported for other herbicide and different adsorbents by others [15,37,52].

3.3. Kinetic and isotherm studies

The adsorption kinetic represents valuable data about efficiency of adsorption, reaction rate and pathway. Among kinetic models, pseudo-first-order and pseudo-second-order models are most commonly used to describe the adsorption. The pseudo-second-order linear plot for the different initial concentrations of bentazon has been depicted in Fig. 10. The estimated kinetic parameters for bentazon have been summarized in Table 2. As revealed in this figure and table, the kinetic data of bentazon adsorption had the best fitting ($R^2 = 0.998$) to pseudo-second-order model. Moreover, when the initial bentazon concentration increased from 10 to 100 mg/L, the value of R^2 for pseudo-second-order model were decreased and the value of q_e increased indicating that adsorption data were in agreement with this model. The results are consistent with previous literatures in which adsorption kinetic of bentazon by different adsorbent were fitted with pseudo-second-order model [51,53].

Adsorption isotherms show how adsorbate molecules distribute between the liquid phase and the solid phase until it reaches the equilibrium state, which is important in optimizing the adsorption process. In the present study, the Langmuir and Freundlich isotherms were applied to the equilibrium data of bentazon adsorption onto CTAB/MMT. Therefore, Freundlich and Langmuir models were analyzed by plotting log (q_e) versus log (C_e) and C_e/q_e versus C_e, respectively (Fig. 11a and b) and the estimated Freundlich and Langmuir constants and related correlation coefficients are given in Table 3. The high correlation coefficient ($R^2 = 0.9936$) confirmed the applicability of the Langmuir model for the bentazon adsorption process onto CTAB/MMT. It means that the adsorption of bentazon onto CTAB/MMT occurred as homogeneous and monolayer phenomena.

The removal capacity of CTAB/MMT is compared in Table 3 to the values reported for different adsorbents [51–58]. As the comparison reveals, the CTAB/MMT sample has effective higher adsorption capacity than the other. Maximum adsorption capacity was obtained 500 mg/g at
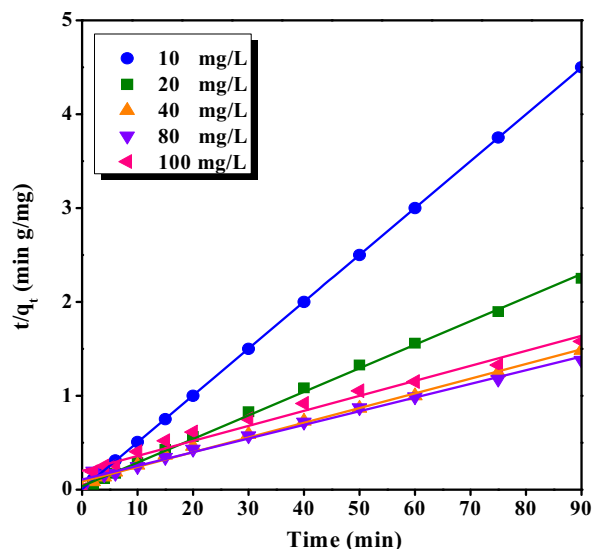
Fig. 10. The linear plots of pseudo-second-order model on the bentazon removal by CTAB/MMT in different time interval (pH = 3, and adsorbent dosage = 0.5 g/L).

pH of 3. Based on the obtained results, the CTAB/MMT can be employed as an efficient and low cost adsorbent for the removal of herbicides.

3.4. Effect of ion strength

Effect of ion strength on the removal efficiency of bentazon by CTAB/MMT was studied in the presence of four different ion compounds. Fig. 12 shows that order of percentage removal of bentazon is sodium carbonate > without anion > sodium bicarbonate > sodium sulfate > sodium chloride. The removed amount of bentazon at initial reaction time in the presence of sodium carbonate was greater than that in the absence of any ions (Fig. 12). Removal percentage of bentazon without presence of any anion increased from 84.34% at 2 min to 99.99% at 90 min. On the other hand, removal percentage of bentazon in the presence of sodium carbonate was increased from 99.45% at 2 min to 99.99% at 90 min. But removal efficiency of bentazon decreased in present of sodium bicarbonate, sodium sulphate, sodium chloride in comparison to without anion.

The bentazon removal was highly decreased in the presence of sodium bicarbonate, sodium sulfate and

Table 2
The calculated kinetic parameters for pseudo-first-order and pseudo-second-order models for removal of herbicide.

[Bentazon]$_0$ (mg/L)	Kinetic model					
	Pseudo-first-order model			Pseudo-second-order model		
	k_1 (1/min)	q_e (mg/g)	R^2	k_2 (g/mg min)	q_e (mg/g)	R^2
10	0.382	19.9	0.841	0.395	20.04	1
20	0.051	40	0.792	0.017	39.84	0.998
40	0.042	62	0.969	0.0028	63.69	0.993
80	0.044	65.89	0.958	0.0021	64.93	0.99
100	0.042	58	0.964	0.0012	62.5	0.97

$$y = 2.029 x - 2.059$$
$$R^2 = 0.9875$$

(a)

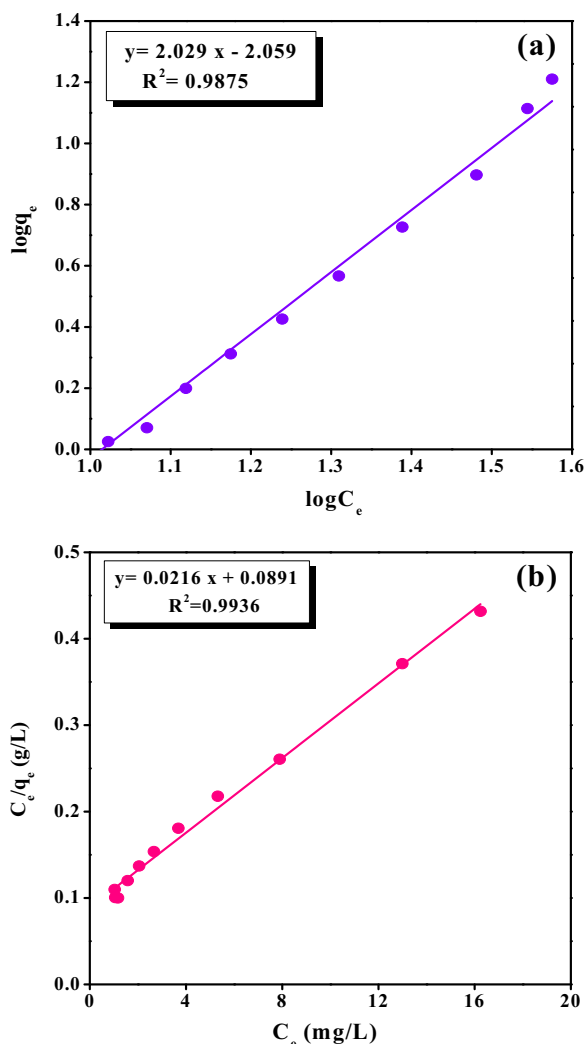$$y = 0.0216 x + 0.0891$$
$$R^2 = 0.9936$$

(b)

Fig. 11. The linear plots of (a) Freundlich isotherm and (b) Langmuir isotherm for bentazon adsorption onto the CTAB/MMT (pH = 3, [Bentazon]$_0$ = 20 mg/L, adsorbent dosage = 0.5 g/L, and time = 24 h).
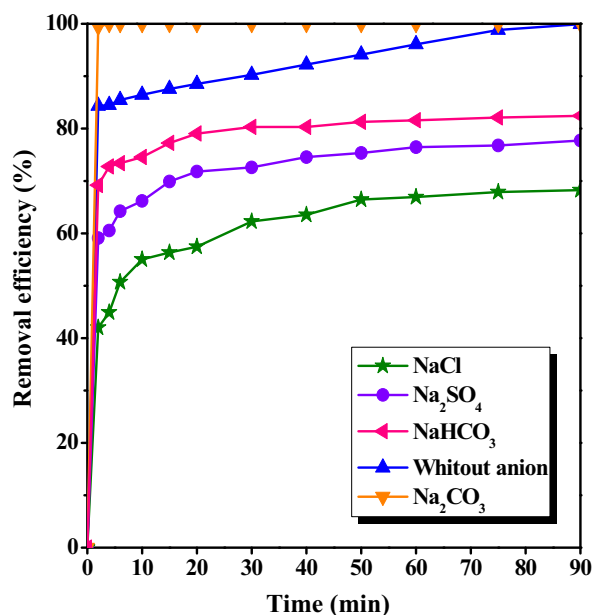

Fig. 12. The effect of ionic strength on the removal of bentazon by CTAB/MMT in different time interval (pH = 3, [Bentazon]$_0$ = 20 mg/L, and adsorbent dosage = 0.5 g/L).

sodium chloride. It was also evident that the removal of bentazon was reduced in the presence of sodium bicarbonate, sodium sulfate and sodium chloride because the adsorption of large bentazon ions mainly depended on the electrical attraction. CO_3^{2-}, Cl^-, and SO_4^{2-} may interfere the electrostatic attraction between SO_3^{2-} ions on bentazon due to the interaction between the surface and added solutes, which may block some of the sorption active sites for the bentazon molecules.

3.5. Comparative study of bentazon removal by MMT and CTAB/MMT

Comparison of between MMT and CTAB/MMT on the adsorption bentazon at initial pH of 3.0 for different time intervals is depicted in Fig. 13. The removal of bentazon
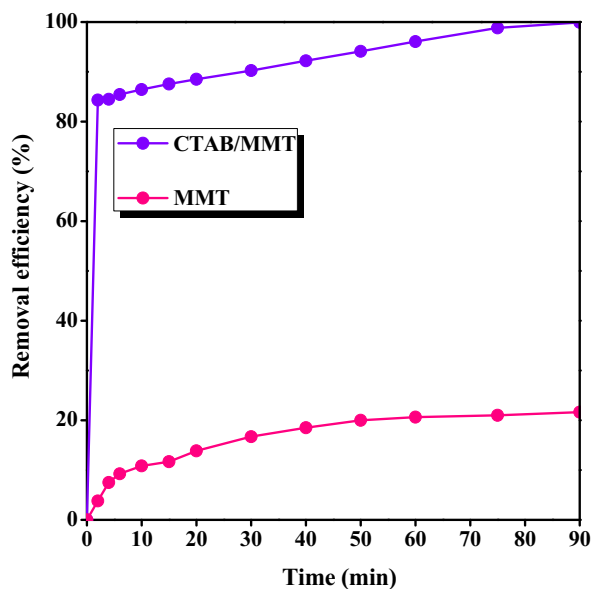
Table 3
The comparison of isotherm constants for the adsorption of herbicides.

Adsorbent	Herbicide name	Langmuir constants			Freundlich constants			Reference
		q_m (mg/g)	K_L (L/mg)	R^2	K_F (mg/g (L/mg)$^{1/n}$)	n	R^2	
Ayous sawdust	Paraquat	36.84	0.0135	0.993	2.9734	2.58	0.97	[54]
Date stone	Aldrin	6.369	2.323	0.913	4.976	1.414	0.994	[55]
Date stone	Dieldrin	6.975	1.401	0.901	3.908	1.435	0.998	[55]
Date stone	Endrin	5.982	0.878	0.924	2.458	1.416	0.998	[55]
Tea leave	Quinalphos	196.07	0.520	0.997	9.4	0.962	0.985	[56]
Date see activated carbon	Bentazon	86.27	0.017	0.968	6.47	1.78	0.975	[53]
Date see activated carbon	Carbofuran	137.04	0.053	0.968	13.07	2.68	0.979	[53]
Lawsonia inermis wood	Bentazon	169.491	0.183	0.996	26.73	1.615	0.934	[51]
Montmorillonite (C10M)	2-4D	5.03	0.02	0.85	0.91	0.067	0.98	[57]
Diatomaceous earth	Paraquat	17.54	1.72	0.859	12.8	0.074	0.949	[58]
Na-montmorillonite SWy-1	3-Chloroaniline	0.096	0.031	0.9211	0.003	0.65	0.9559	[52]
Na-montmorillonite SWy-1	4-Chlorophenol	0.174	0.22	0.8593	0.02	1.068	0.9473	[52]
CTAB/MMT	Bentazon	500	0.225	0.9936	12271.5	3.253	0.9885	Present study

Fig. 13. Comparison of removal efficiency between MMT and CTAB/MMT on the bentazon removal in different time interval (pH = 3, [Bentazon]$_0$ = 20 mg/L, and adsorbent dosage = 0.5 g/L).

was low in the presence of MMT. However, in the presence of CTAB/MMT 99.99% of the bentazon was eliminated at the time of 90 min. Chemical modification of pure MMT with an appropriate chemical agent also CTAB would be favourable to reach suitable surface charge in order to increase adsorption capacity of the clay.

4. Conclusions

In the present research, the application of MMT modified with CTAB for adsorption of the bentazon in aqueous solutions was studied. The prepared sample was characterized by of FT–IR, XRD, SEM and EDX. The results indicated more adsorption activity of the MMT modified with CTAB in comparison with unmodified MMT. The removal efficiency depended on experimental parameters like the amount of CTAB/MMT, contact time, pH and initial bentazon concentration. The removal efficiency at optimum pH 3 was found to increase with increase in contact time and adsorption dosage, but to decrease with increase in initial bentazon concentration. Analysis of CTAB/MMT by FT–IR, XRD, SEM and EDX revealed functional groups, porous surface and abundant cation elements that contribute to the bentazon adsorption. Pseudo-second-order model described the adsorption kinetics of bentazon onto CTAB/MMT better than first one. The high value of correlation coefficient ($R^2 = 0.9936$) for the Langmuir isotherm pointed out that adsorption was occurred on homogeneous and monolayer surface. According to the obtained results, the maximum adsorption capacity for bentazon was 500 mg/g.

Acknowledgments

References

[1] M.H. Thembela Hillie, Nat. Nanotechnol. 2 (2007) 663.
[2] R.A. Rebich, R.H. Coupe, E.M. Thurman, Sci. Total Environ. 321 (2004) 189.
[3] H. Azejjel, C. del Hoyo, K. Draoui, M.S. Rodríguez-Cruz, M.J. Sánchez-Martín, Desalination 249 (2009) 1151.
[4] J.M. Salman, B.H. Hameed, J. Hazard. Mater. 175 (2010) 133.
[5] E. Ayranci, N. Hoda, Chemosphere 60 (2005) 1600.
[6] J. Da Silva Coelho, A.L. De Oliveira, C.G. Marques de Souza, A. Bracht, R.M. Peralta, Int. Biodeter. Biodegr. 64 (2010) 156.
[7] World Health Organization, Guidelines for Drinking-Water Quality, Third ed., 2004.
[8] J.M. Salman, V.O. Njoku, B.H. Hameed, Chem. Eng. J. 174 (2011) 41.
[9] A.L. De Castro Peixoto, A.C.S.C. Teixeira, J. Photochem. Photobiol. A 275 (2014) 54.
[10] R. Pourata, A.R. Khataee, S. Aber, N. Daneshvar, Desalination 249 (2009) 301.
[11] E. Brillas, P.-L. Cabot, R.M. Rodríguez, C. Arias, J.A. Garrido, R. Oliver, Appl. Catal. B: Environ. 51 (2004) 117.
[12] M.V. Shankar, S. Anandan, N. Venkatachalam, B. Arabindoo, V. Murugesan, Chemosphere 63 (2006) 1014.
[13] Y. Zhang, Y. Hou, F. Chen, Z. Xiao, J. Zhang, X. Hu, Chemosphere 82 (2011) 1109.
[14] V.K.G. Imran Ali, Nat. Protoc. 1 (2007) 2661.
[15] E. Ayranci, N. Hoda, Chemosphere 57 (2004) 755.
[16] S.K. Alpat, Ö. Özbayrak, Ş Alpat, H. Akçay, J. Hazard. Mater. 151 (2008) 213.
[17] A. Hassani, L. Alidokht, A.R. Khataee, S. Karaca, J. Taiwan Inst. Chem. Eng. 45 (2014) 1597.
[18] A. Hassani, F. Vafaei, S. Karaca, A.R. Khataee, J. Ind. Eng. Chem. 20 (2014) 2615.
[19] N. Daneshvar, S. Aber, A. Khani, A.R. Khataee, J. Hazard. Mater. 144 (2007) 47.
[20] C.-F. Chang, S.-C. Lee, Water Res. 46 (2012) 2869.
[21] M. Imamoglu, O. Tekir, Desalination 228 (2008) 108.
[22] M.J. Sanchez-Martin, M.S. Rodriguez-Cruz, M.S. Andrades, M. Sanchez-Camazano, Appl. Clay Sci. 31 (2006) 216.
[23] S.-J. Park, Y.-S. Jang, J. Colloid. Interf. Sci. 249 (2002) 458.
[24] S.L. Neitsch, K.J. McInnes, S.A. Senseman, G.N. White, E.E. Simanek, Chemosphere 64 (2006) 704.
[25] O.R. Pal, A.K. Vanjara, Sep. Purif. Technol. 24 (2001) 167.
[26] J. Li, Y. Li, J. Lu, Appl. Clay Sci. 46 (2009) 314.
[27] M. Cruz-Guzmán, R. Celis, M.C. Hermosín, J. Cornejo, Environ. Sci. Technol. 38 (2003) 180.
[28] A. Marsal, E. Bautista, I. Ribosa, R. Pons, M.T. García, Appl. Clay Sci. 44 (2009) 151.
[29] L. Zhang, L. Luo, S. Zhang, Colloid. Surf. A 377 (2011) 278.
[30] F. Rasouli, S. Aber, D. Salari, A.R. Khataee, Appl. Clay Sci. 87 (2014) 228.
[31] G. Akçay, M. Akçay, K. Yurdakoç, J. Colloid. Interf. Sci. 296 (2006) 428.
[32] S. Karaca, A. Gürses, Ö. Açışlı, A. Hassani, M. Kıranşan, K. Yıkılmaz, Desalin. Water Treat. 51 (2013) 2726.
[33] M. Terce, R. Calvet, Chemosphere 7 (1978) 365.
[34] Y. Park, Z. Sun, G.A. Ayoko, R.L. Frost, J. Colloid. Interf. Sci. 415 (2014) 127.
[35] A. Cabrera, C. Trigo, L. Cox, R. Celis, M.C. Hermosin, J. Cornejo, W.C. Koskinen, Eur. J. Soil Sci. 63 (2012) 694.
[36] R. Celis, C. Trigo, G. Facenda, M.D.C. Hermosín, J. Cornejo, J. Agr. Food Chem. 55 (2007) 6650.
[37] Y. El-Nahhal, J. Environ. Sci. Heal. B 38 (2003) 591.
[38] M.J. Rosen, Surfactants and Interfacial Phenomena, John Wiley & Sons, Inc., USA, 1978.
[39] L. Margulies, H. Rozen, S. Nir, Clay. Clay Miner. 36 (1988) 270.
[40] A.R. Khataee, F. Vafaei, M. Jannatkhah, Int. Biodeter. Biodegr. 83 (2013) 33.
[41] R. Darvishi Cheshmeh Soltani, A.R. Khataee, M. Safari, S.W. Joo, Int. Biodeter. Biodegr. 85 (2013) 383.
[42] E. Daneshvar, M. Kousha, M.S. Sohrabi, A. Khataee, A. Converti, Chem. Eng. J. 195–196 (2012) 297.
[43] I. Langmuir, J. Am. Chem. Soc. 40 (1918) 1361.
[44] H.M.F. Freundlich, J. Phys. Chem. A 57 (1906) 385.
[45] A.K. Mishra, S. Allauddin, R. Narayan, T.M. Aminabhavi, K.V.S.N. Raju, Ceram. Int. 38 (2012) 929.

[46] J. Madejová, Vib. Spectrosc. 31 (2003) 1.
[47] Y. Ma, J. Zhu, H. He, P. Yuan, W. Shen, D. Liu, Spectrochim. Acta A 76 (2010) 122.
[48] M. Xia, Y. Jiang, F. Li, M. Sun, B. Xue, X. chen, Colloid. Surf. A 338 (2009) 1.
[49] S. Karaca, A. Gürses, M. Ejder Korucu, J. Chem. (2013) 1.
[50] A. Boivin, R. Cherrier, M. Schiavon, Chemosphere 61 (2005) 668.
[51] A. Omri, A. Wali, M. Benzina, Arab. J. Chem (2012), http://dx.doi.org/10.1016/j.arabjc.2012.04.047.
[52] S. Polati, F. Gosetti, V. Gianotti, M.C. Gennaro, J. Environ. Sci. Health B 41 (2006) 765.
[53] J.M. Salman, V.O. Njoku, B.H. Hameed, Chem. Eng. J. 173 (2011) 361.
[54] C.P. Nanseu-Njiki, G.K. Dedzo, E. Ngameni, J. Hazard Mater. 179 (2010) 63.
[55] H. El Bakouri, J. Usero, J. Morillo, R. Rojas, A. Ouassini, Bioresource Technol. 100 (2009) 2676.
[56] M.A. Islam, V. Sakkas, T.A. Albanis, J. Hazard Mater. 170 (2009) 230.
[57] M.C. Hermosin, J. Cornejo, Chemosphere 24 (1992) 1493.
[58] W.T. Tsai, K.J. Hsien, Y.M. Chang, C.C. Lo, Bioresour. Technol. 96 (2005) 657.